

Fabrication of large all-PDMS micropatterned waveguides for lab on chip integration using a rapid prototyping technique

DANIEL PÉREZ-CALIXTO,^{1,2} DIEGO ZAMARRÓN-HERNÁNDEZ,¹ AARÓN CRUZ-RAMÍREZ,¹ MATHIEU HAUTEFEUILLE,^{1,*} JUAN HERNÁNDEZ-CORDERO,³ VÍCTOR VELÁZQUEZ,¹ AND MARCELA GREYER¹

¹Facultad de Ciencias, Universidad Nacional Autónoma de México, México

²Posgrado de Ciencia e Ingeniería de Materiales, Universidad Nacional Autónoma de México, México

³Instituto de Investigaciones en Materiales, Universidad Nacional Autónoma de México, México

*mathieu_h@ciencias.unam.mx

Abstract: A simple method for manufacturing centimeter-long all-PDMS embedded and rib microwaveguides is presented. It allows for the fabrication of centimeter-long micromolds by direct laser ablation of a desired waveguide pattern inside an acrylic sheet to create a pattern which is then transferred to a poly-dimethylsiloxane (PDMS) layer using soft-lithography. A refractive index difference between the core and cladding of 1.3×10^{-3} was achieved by controlling the PDMS curing and linear attenuation of 1.27 dB/cm for embedded and 2.36 dB/cm for a rib waveguide, similar to other techniques. Finally, a beamsplitter was fabricated to demonstrate that our low-cost process is suitable to integrate waveguide devices on lab on chip platforms.

© 2017 Optical Society of America

OCIS codes: (220.0220) Optical design and fabrication; (230.0230) Optical devices; (160.0160) Materials.

References and links

1. M. J. Madou, *Fundamentals of Microfabrication: The Science of Miniaturization* (CRC Press, 2002).
2. R. Zaouk, B. Y. Park, and M. J. Madou, *Introduction to Microfabrication Techniques in Microfluidic Techniques*, Shelley D. Minter, ed. (Humana Press Inc, 2006).
3. C. R. Martin and I. A. Aksay, "Microchannel molding: A soft lithography inspired approach to micrometer-scale patterning," *J. Mater. Res.* **20**(08), 1995–2003 (2005).
4. M. Röhrig, M. Thiel, M. Worgull, and H. Hölscher, "3D direct laser writing of nano- and microstructured hierarchical gecko-mimicking surfaces," *Small* **8**(19), 3009–3015 (2012).
5. X. Fan, I. M. White, S. I. Shopova, H. Zhu, J. D. Suter, and Y. Sun, "Sensitive optical biosensors for unlabeled targets: A Review," *Anal. Chim. Acta* **620**(1-2), 8–26 (2008).
6. A. Ksendzov and Y. Lin, "Integrated optics ring-resonator sensors for protein detection," *Opt. Lett.* **30**(24), 3344–3346 (2005).
7. S. Hengsbach and A. D. Lantada, "Rapid prototyping of multi-scale biomedical microdevices by combining additive manufacturing technologies," *Biomed. Microdevices* **16**(4), 617–627 (2014).
8. K. B. Mogensen, H. Klank, and J. P. Kutter, "Recent developments in detection for microfluidic systems," *Electrophoresis* **25**(21-22), 3498–3512 (2004).
9. H. Nishi, T. Tsuchizawa, R. Kou, H. Shinjima, T. Yamada, H. Kimura, Y. Ishikawa, K. Wada, and K. Yamada, "Monolithic integration of a silica AWG and Ge photodiodes on Si photonic platform for one-chip WDM receiver," *Opt. Express* **20**(8), 9312–9321 (2012).
10. W. Bogaerts, P. De Heyn, T. Van Vaerenbergh, K. De Vos, S. Kumar Selvaraja, T. Claes, P. Dumon, P. Bienstman, D. Van Thourhout, and R. Baets, "Silicon microring resonators," *Laser Photonics Rev.* **6**(1), 47–73 (2011).
11. Y. Zhang, S. Yang, A. E. Lim, G. Q. Lo, C. Galland, T. Baehr-Jones, and M. Hochberg, "A compact and low loss Y-junction for submicron silicon waveguide," *Opt. Express* **21**(1), 1310–1316 (2013).
12. J. S. Kee, D. P. Poenar, P. Neuzil, and L. Yobas, "Monolithic integration of poly(dimethylsiloxane) waveguides and microfluidics for on-chip absorbance measurements," *Sens. Actuators B Chem.* **134**(2), 532–538 (2008).
13. K. S. Lee, H. L. T. Lee, and R. J. Ram, "Polymer waveguide backplanes for optical sensor interfaces in microfluidics," *Lab Chip* **7**(11), 1539–1545 (2007).
14. P. Fei, Z. Chen, Y. Men, A. Li, Y. Shen, and Y. Huang, "A compact optofluidic cytometer with integrated liquid-core/PDMS-cladding waveguides," *Lab Chip* **12**(19), 3700–3706 (2012).

15. D. A. Chang-Yen and B. K. Gale, "An Integrated Optical Glucose Sensor Fabricated Using PDMS Waveguides on a PDMS," *Proc. SPIE* **5345**, 98–107 (2004).
16. L. Novak, P. Neuzil, J. Pipper, Y. Zhang, and S. Lee, "An integrated fluorescence detection system for lab-on-a-chip applications," *Lab Chip* **7**(1), 27–29 (2007).
17. D. A. Chang-yen, R. K. Eich, and B. K. Gale, "A monolithic PDMS waveguide system fabricated using soft-lithography techniques," *J. Lightwave Technol.* **23**(6), 2088–2093 (2005).
18. J. S. Kee, D. P. Poenar, P. Neuzil, and L. Yobas, "Design and fabrication of poly(dimethylsiloxane) single-mode rib waveguide," *Opt. Express* **17**(14), 11739–11746 (2009).
19. Z. Cai, W. Qiu, G. Shao, and W. Wang, "A new fabrication method for all-PDMS waveguides," *Sens. Actuators A Phys.* **20**(204), 44–47 (2013).
20. R. Horváth, L. R. Lindvold, and N. B. Larsen, "Fabrication of all-polymer freestanding waveguides," *J. Micromech. Microeng.* **13**(3), 419–424 (2003).
21. Y. Xia and G. M. Whitesides, "Soft Lithography," *Annu. Rev. Mater. Sci.* **28**(1), 153–184 (1998).
22. H. Hosseinkhannazer, L. W. Kostiuik and J.N. McMullin, "Two-species microparticle detection in optofluidic biochips with polymeric waveguides," *Proc. SPIE* **7099**, 70990H (2008).
23. J. Missinne, E. Bosman, B. Van Hoe, G. Van Steenberge, S. Kalathimekkad, P. Van Daele, and J. Vanfleteren, "Flexible Shear Sensor Based on Embedded Optoelectronic Components," *IEEE Photonics Technol. Lett.* **23**(12), 771–773 (2011).
24. X. Zhang, W. Que, J. Chen, J. Hu, T. Gao, and W. Liu, "Sol-gel concave micro-lens arrays fabricated by combining the replicated PDMS soft mold with UV-cured imprint process," *Appl. Phys. B* **113**(2), 299–306 (2013).
25. S. Kopetz, D. Cai, E. Rabe, and A. Neyer, "PDMS-based optical waveguide layer for integration in electrical-optical circuit boards," (AEU)," *Int. J. Electron. Commun.* **61**(3), 163–167 (2007).
26. S. K. Sia and G. M. Whitesides, "Microfluidic devices fabricated in poly(dimethylsiloxane) for biological studies," *Electrophoresis* **24**(21), 3563–3576 (2003).
27. S. M. Azmayesh-Fard, E. Flaim, and J. N. McMullin, "PDMS biochips with integrated waveguides," *J. Micromech. Microeng.* **20**(8), 087002 (2010).
28. P. Fei, Z. Chen, Y. Men, A. Li, Y. Shen, and Y. Huang, "A compact optofluidic cytometer with integrated liquid-core/PDMS-cladding waveguides," *Lab Chip* **12**(19), 3700–3706 (2012).
29. D. Jandura, D. Pudis, and S. Berezina, "Photonic devices prepared by embossing in PDMS," *Appl. Surf. Sci.* **395**(1), 145–149 (2016).
30. L. Cabriaes, M. Hautefeuille, G. Fernández, V. Velázquez, M. Grether, and E. López-Moreno, "Rapid fabrication of on-demand high-resolution optical masks with a CD-DVD pickup unit," *Appl. Opt.* **53**(9), 1802–1807 (2014).
31. D. Melati, A. Melloni, and F. Morichetti, "Real photonic waveguides: guiding light through imperfections," *Adv. Opt. Photonics* **6**(2), 156–224 (2014).
32. I. Martinček, I. Turek, and N. Tarjányi, "Effect of boundary on refractive index of PDMS," *Opt. Mater. Express* **4**(10), 1997–2005 (2014).

1. Introduction

In recent years, interest in microscale devices has grown due to the wide range of applications available with the advent of microtechnology. Multifunctional integrated design for lab on a chip (LoC) platforms is an example of a technology that is currently being pursued, owing to the increased control and availability of fabrication processes for tridimensional micron-scale patterns. These in turn have opened new routes for fabricating functional platforms with on-demand complex geometries in a variety of materials, integrating all the necessary elements for manipulation and analysis, thereby reducing the overall costs and fabrication time [1]. Thanks to photolithography [2], soft-lithography [3] and laser fabrication techniques [4], designs with micrometric dimensions can also be integrated on chip to help enabling greater sensitivities and resolutions in critical applications such as diagnostics biosensors and therapeutic systems. These may lead to high-impact commercial solutions provided that the manufacturing processes are reproducible [5,6]. For applications requiring lower-cost solutions, microtechnology is also providing rapid-prototyping techniques adapted to remote-access, point-of-care devices that may even be fabricated on site following a simple procedure [7,8].

Optical signals are often sought as an attractive characteristic in lab-on-chip devices or portable optoelectronics circuits. Integration at the micron scale of beamsplitters, interferometers, resonators, multiplexers and waveguides has proven useful in many applications requiring such capabilities [9–11]. Also, designing waveguides for efficient light coupling is important to avoid the need of external alignment tools that are difficult to

manipulate at microscale. Furthermore, waveguides are key elements to couple light into microfluidic systems as well as for superficial bioanalyte detection schemes [12,13]. Waveguide design and fabrication can be complex and challenging for such purposes, in particular for structures intended to couple light from the chip to external readout equipment [14–16].

Mature processes to develop custom-built, integrated optical waveguides with micron scale resolution typically use photolithography for micropatterning or laser direct writing for local modification of the refractive index [2–4]. When polymers are needed for lab on chip applications, soft lithography is compatible with these materials, but the master micromolds used in these processes also presuppose microelectronics-based costly equipment, as well as a controlled environment [17–19]. However, these technologies are not always compatible with the modern needs for custom-made, rapid-prototyping solutions required in LoC mostly due to their limited accessibility. Moreover, they are also less versatile if small volumes or single-chip production are required. The choice of materials is also an important consideration for device development. Recent trends for polymer-based microchips are currently requiring methods that are compliant with materials other than silicon and glass [20]. As an example, poly-dimethylsiloxane (PDMS) is a very popular cost effective material used in LoC since Whitesides and Xia presented soft-lithography recipes for microchips construction with widespread usage [21]. It has also been used successfully in micro-optoelectronics applications [22–24] owing to its interesting mechanical, thermal and optical properties that can be exploited simultaneously. Since PDMS is transparent in the UV-visible range (230 nm - 700 nm) [25–27], it is also used for waveguide fabrication, either as a high refractive index filler for micromachined shallow channels [18,28], or as a micropatterned substrate filled with a lower-index material [20]. As in any soft-lithography process, PDMS-based waveguide fabrication relies heavily on the availability of a micromold. Hence, the fabrication of microstructured master molds with the required waveguide features is a critical step in this case.

In this work, we present a simple rapid-prototyping method to fabricate all-PDMS micro-waveguides making use of another interesting property of this material: the dependence of its refractive index on the curing temperature and the prepolymer-curing agent mixing proportions [17,19]. Similar approaches have been shown in previous works, but the cost of obtaining centimeter-range dimensions for the resulting waveguides is typically elevated for a photolithography mold [17,19,29]. Our method allows for the fabrication of centimeter-long micromolds by direct laser ablation of a desired waveguide pattern inside an acrylic sheet. This is achieved using a low-cost CD-DVD optical pickup head system reported previously [30]. The micromolds are then filled with PDMS with the proper refractive indices to form waveguides. Light propagation through these waveguides is successfully demonstrated, hence validating the fabrication process as a viable method for the fabrication of centimeter-long polymer waveguides. Furthermore, we also show that our low-cost, rapid prototyping direct laser writing of molds allows for the simple fabrication of devices such as beam splitters, yielding repeatable results and suitable for lab-on-chip applications.

2. Methodology and fabrication process

Our fabrication process is based on a soft-lithography replica-molding method entailing the steps depicted in Fig. 1 [21]. First, a computer is used to design the waveguide as a bitmap (1) that is then transferred to a Computer Numerical Control (CNC) laser system. This uses a CD-DVD pickup head to etch the desired design on the surface of an acrylic sheet (2), following a procedure similar to that described in [30]. Carbon nanoparticles (Sigma Aldrich, #633100) are used to coat the surface of the transparent substrate in order to enable etching at low laser power of this otherwise non-absorbing material, thus yielding the mold that is characterized using profilometry (3). PDMS (Sylgard 184, Dow Corning) is then prepared by motor-mixing the prepolymer and curing agent in a 5:1 w/w proportion and pouring it inside

the negative of the waveguide of the mold channel (4). Special attention is paid to the mixing process and the desiccating times to ensure process reproducibility. Excess of PDMS is carefully removed from the mold surface (5) and the sample is cured at 60°C for 4h in a convection oven (6). A 20:1 w/w PDMS mixture is then prepared and poured onto the sample which is subsequently cured at room temperature for 48h (7) to avoid any possible deformation or physical mismatch between the PDMS layers as well as to ensure refractive index homogeneity and to minimize possible ageing effects that may arise when the curing process is carried out over short periods of time. After curing, the PDMS slab, consisting of a 20:1 substrate and a 5:1 step guide, is removed from the mold (9) and covered with another 20:1 w/w ratio PDMS mixture that is cured at room temperature for 48h (10). According to the literature, these proportions of prepolymer and curing agent yield a larger refractive index for the mixture of the core, hence enabling light confinement within the resulting waveguide structure [31].

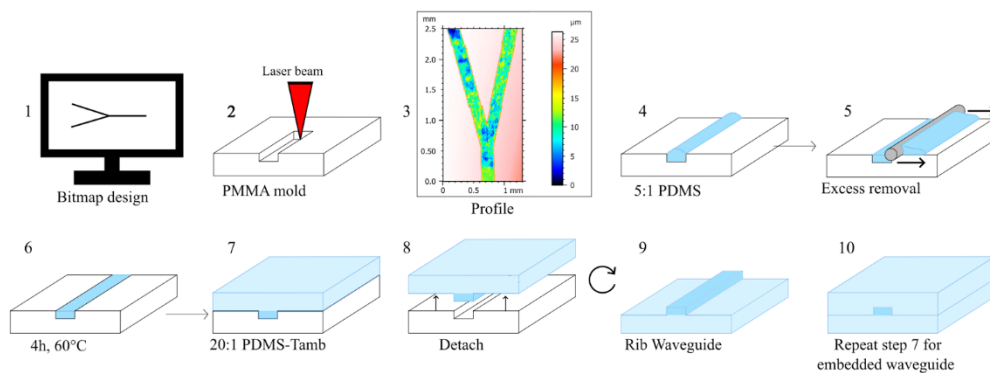


Fig. 1. All-PDMS waveguides fabrication procedure as described in the text.

In contrast to the extended curing time, the preparation of the different layers of PDMS requires only a couple of hours. Both time frames provide an effective means to produce all-PDMS microwaveguides in a scalable fashion.

3. Characterization

First, the microstructured molds were characterized by profilometry (KLA-Tencor D600) to verify the dimensions of the designed structures. Using this technique, we were also able to address roughness of the channel to be filled with PDMS (5:1 ratio, see Fig. 1). Optical microscopy was further used to evaluate the profiles of the channels.

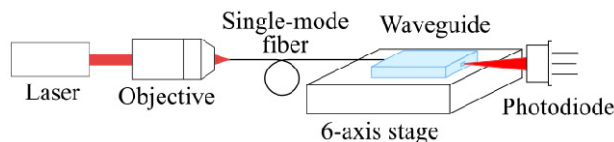


Fig. 2. Diagram of the optical setup used for optical waveguides characterization.

The refractive index of all samples obtained with the different PDMS mixture ratios was measured after curing with a Metricon Prism Coupler system. Measurements were taken at five positions for three samples and on different days. The resulting values were then averaged to obtain a nominal refractive index. Following this characterization method, we were able to verify that the preparation procedure yielded consistent and repeatable refractive indices for the PDMS samples. Furthermore, we were able to assess the homogeneity of the refractive index throughout the samples.

In order to validate our process for the fabrication of all-PDMS waveguides, two designs were realized. Straight waveguides with different lengths (1 cm, 1.5 cm, 2 cm and 2.5 cm), as well as a fully embedded beamsplitter (“Y” shape); both designs were carried out using image editor software. The resulting waveguides were characterized using the setup depicted in Fig. 2. The output from a laser diode (638.22 nm) was coupled to a single-mode optical fiber with an NA of 0.13 and a cutoff wavelength of 570 ± 30 nm, via a 20X microscope objective. The output end of the fiber was coupled to the all-PDMS waveguide chips under test. Light coupling into the waveguides was optimized upon aligning the fiber tip with the PDMS core by means of a 6-axis stage.

Optical propagation losses are a very important parameter to evaluate the performance of a waveguide. These may arise from different factors such as material intrinsic absorption, geometry, scattering due to boundary roughness as well as other fabrication defects and imperfections [31]. The optical losses in our waveguides were evaluated using the cutback method, as reported in [17,18]. An optical power meter (Thorlabs PM100) and a silicon photodiode (Thorlabs S120VC) were used for this purpose; as customary, the waveguide attenuation was estimated as:

$$\alpha L = -10 \text{Log} \left(\frac{P_1}{P_0} \right) \quad (1)$$

where α is the attenuation coefficient, L is the waveguide length, P_1 and P_0 as the optical power measured at the output and input respectively. The numerical aperture “NA” and acceptance angle θ_a of the waveguides was also estimated from the measured values of refractive indices. The numerical aperture is given by.

$$NA = \sqrt{n_c^2 - n_s^2} \quad (2)$$

where n_c is the core refractive index of the core and n_s is that of the surrounding medium (cladding), whereas the acceptance angle is estimated with the numerical aperture and the refractive index of the external medium n_1 :

$$\theta_a = \sin^{-1} \left(\frac{NA}{n_1} \right) \quad (3)$$

4. Experimental results

We first measured the refractive index of each PDMS mixture ratio in order to assess the index differences attainable with each blend. After curing, the mixtures prepared with a 5:1 ratio yielded an average refractive index of 1.4113 (± 0.0002), while the PDMS with a 20:1 weight ratio had a lower index of 1.4100 (± 0.0002). The resulting index difference between both mixtures (1.3×10^{-3}) can therefore provide a viable platform for light confinement if the blends are adequately used to form the core and the cladding of a waveguide. These measurements were carried out several times and in different seasons throughout the year to verify the repeatability of the curing process. We did not find significant variations in the index contrast thus evidencing that the proposed methodology yields reproducible results for preparing PDMS structures with refractive indices suitable for waveguide fabrication. For the fabricated waveguides, we obtained that $NA = 0.0605$ and $\theta_a = 2.45942^\circ$, suggesting that a very good control of alignment is required for the light to be coupled into the chip.

Figure 3(a)-3(b) shows typical side view micrographs of two different all-PDMS straight waveguides. These were fabricated using the method depicted in Fig. 1. The rib of the waveguide was formed using the 5:1 ratio PDMS, and it is sitting on a lower refractive index (20:1 ratio) PDMS layer Fig. 3(b). A waveguide having a 5:1 ratio PDMS core embedded waveguide in a 20:1 ratio PDMS cladding is shown in Fig. 3(a). It is clear that our laser

ablation process is leaving small roughnesses at the bottom of the acrylic micromolds; as seen in the Figs., these imperfections are replicated into the rib and channel. Using profilometry, we were able to scan the full surface of the fabricated structures yielding an average roughness of $4.51 \pm 1.26 \mu\text{m}$ for the full strip for two different 2 centimeter long samples.

The attenuation measurements for the waveguides are shown in Fig. 3(c) and 3(d). While the embedded waveguide showed a 1.27 dB/cm attenuation, the rib waveguide yielded a 2.36 dB/cm attenuation. Both had dimensions of 1.928 cm of initial length, $90.0 (\pm 2.4) \mu\text{m}$ in width and $39.6 (\pm 5.9) \mu\text{m}$ in depth, as measured with the profilometer. Although our chips are made of slightly rough centimeter-long channels, the results are similar to those reported in the literature for micro-waveguides [17,19]. Clearly, the embedded waveguides are a better option for such LoC applications, owing to their small propagation losses compared to those obtained for the rib structure. This difference in losses between both structures is due to the different guiding mechanisms involved in each waveguide architecture [32].

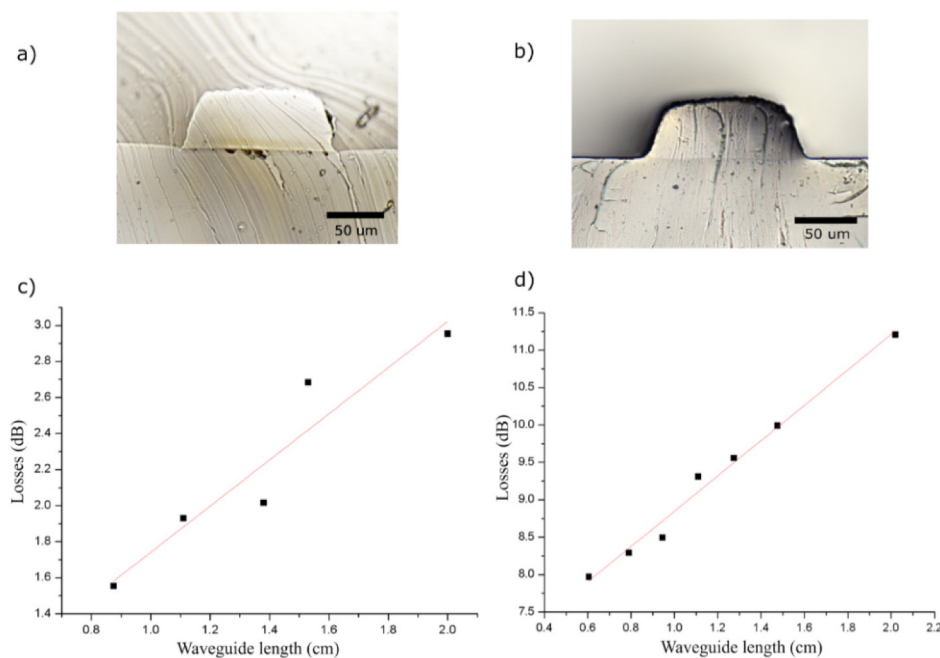


Fig. 3. Side view micrograph of all-PDMS waveguides: (a) embedded channel, and (b) rib waveguide. Both structures were cut perpendicularly to the propagation axis. Measurements of optical attenuation for: (c) embedded and (d) rib waveguides. The lines in the plots represent the linear fitting of the experimental points, showing an attenuation of 1.27dB/cm for the embedded channel and 2.36dB/cm for the rib waveguide.

In order to evaluate the capabilities of our fabrication method, an embedded beamsplitter was fabricated as a proof-of-concept for waveguide devices. In this case, an 8 mm long “Y” shaped beamsplitter was fabricated; the theoretical acceptance angle for the index contrast was considered to design the device, resulting in an angle of 13° between each of the arms Fig. 4. The separation between the arms of the splitter was set to 1 mm in order to easily discriminate between both outputs, as seen in Fig. 4. Using the profilometer, the channels were measured to be $200 (\pm 2.55) \mu\text{m}$ wide, with a depth of $15 (\pm 1) \mu\text{m}$ and a roughness of $1.2 (\pm 0.5) \mu\text{m}$, both averaged over the full pattern. The performance of the chip was evaluated upon coupling the 638 nm laser into the beam splitter and a single-mode optical fiber was used for light launching ($3.5/125 \mu\text{m}$ core/cladding diameter, 0.13 NA). With this setup, it was possible to manipulate the position and angle of the fiber with respect to the

waveguide input, which in turn enabled both, coupling and full switching between both arms of the device.

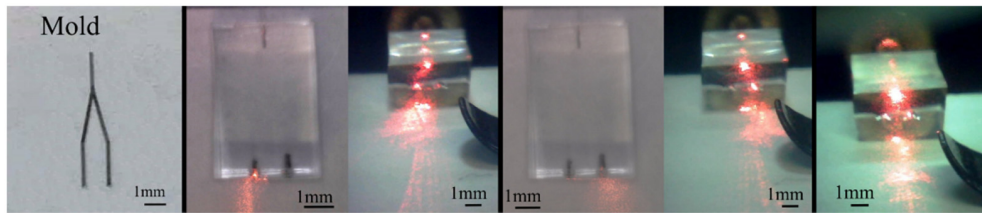


Fig. 4. Beamsplitter validation test design. Separation between the legs with respect to the central input channel is controlled to vary the output efficiency as it is getting closer to the critical angle.

It is clear from the results shown in Fig. 4 that the fabricated beamsplitter separates the beam into both of the output arms. The optical intensity exiting the arms was observed to depend on the coupling conditions of the input beam. Upon varying the between the optical fiber and the waveguide chip, it was also possible to obtain full switching of the output light between both arms.

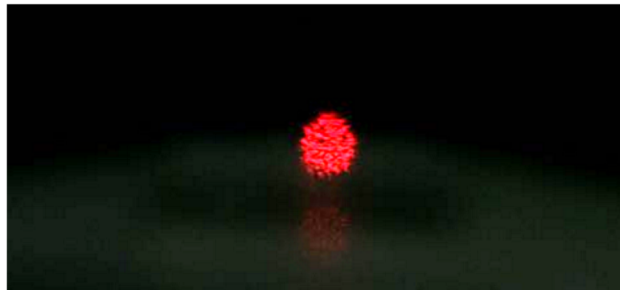


Fig. 5. Speckle pattern observed at a small distance from the output of a 2 cm long straight embedded waveguide chip.

In general, the resulting all-PDMS waveguides are multimode, as evidenced from the speckle patterns registered with a CCD camera at the output end of the chips. Figure 5 shows a typical speckle pattern obtained at the output end of a 2 cm long straight waveguide chip. Considering the dimensions of the waveguide and the index contrast of the PDMS mixtures, we estimate that these structures can support ~ 1000 modes.

5. Conclusions

We have demonstrated a simple, cost-effective fabrication technique for long all-PDMS waveguides. The proposed methodology is compatible with the rapid prototyping development of lab on chip devices and thus has the potential for enabling the easy integration of optical elements in PDMS platforms. The refractive index of PDMS was tailored by modifying the curing temperature and curing agent-prepolymer ratio in order to obtain an index difference of 1.3×10^{-3} , thereby enabling light guiding within the all-PDMS structures. Our method has proven to be very effective to fabricate reproducible chips with any desired pattern in only a couple of hours. We believe it is an interesting solution to enable the integration of optoelectronics and optofluidics into lab on chip in the future.

Funding

The authors would like to thank DGAPA-UNAM PAPIIT projects TA100315, IT101215 and IN116914 as well as CONACyT project #246988 for funding.

Acknowledgments

We also thank Erick Flores-Romero from Instituto de Física, UNAM for his kind help in refractive index measurements.